2014

# Homocysteine intensifies embryonic LIM3 expression in migratory neural crest cells: A quantitative confocal microscope study

Jordan Naumann
*University of Northern Iowa*

# HOMOCYSTEINE INTENSIFIES EMBRYONIC LIM3 EXPRESSION IN MIGRATORY NEURAL CREST CELLS – A QUANTITATIVE CONFOCAL MICROSCOPE STUDY

An Abstract of a Thesis

Submitted

in Partial Fulfillment

of the Requirements for the Degree

Master of Science

Jordan Naumann

University of Northern Iowa

May 2014

ABSTRACT

Elevated levels of homocysteine in maternal blood and amniotic fluid are associated with cardiovascular, renal, skeletal, and endocrine diseases and also with embryonic malformations related to neural crest cells. Neural crest cells are necessary for the formation of tissues and organs throughout the body of vertebrate animals. The migration of neural crest cells is essential for proper development of the target tissues. When migration is disrupted, abnormalities may occur. Migration is affected by transcriptional factor LIM3 protein, which regulates the dynamic components of the neural crest cell cytoskeleton.

The objective of this study was to test the hypothesis that exogenous homocysteine would induce greater LIM3 protein expression in neural crest cells. We predicted homocysteine increases the expression of LIM3 protein in migrating neural crest cells, causing improper assembly and organization of actin filaments during cellular migration.

We dissected homocysteine treated and control chick embryos at developmental stage 15. The explants were immunostained and sectioned on to slides. We found that the expression of LIM3 protein was significantly enhanced in the areas surrounding the neural tube, the pharynx, and in the periocular mesenchyme of embryos that were subjected to elevated plasma homocysteine when compared to control embryos. Our results support that homocysteine can enhance or alter the migration and behavior or neural crest cells by affecting the cytoskeleton regulation of LIM3 protein.

# HOMOCYSTEINE INTENSIFIES EMBRYONIC LIM3 EXPRESSION IN MIGRATORY NEURAL CREST CELLS – A QUANTITATIVE CONFOCAL MICROSCOPE STUDY

A Thesis

Submitted

in Partial Fulfillment

of the Requirements for the Degree

Master of Science

Jordan Naumann

University of Northern Iowa

May 2014

This Study by: Jordan Naumann

Entitled: Homocysteine Intensifies Embryonic LIM3 Expression in Migratory Neural Crest Cells--a Quantitative Confocal Microscope Study

has been approved as meeting the thesis requirement for the

Degree of Master of Science

| | |
|---|---|
| _____ | _____ |
| Date | Dr. Darrell Wiens, Chair, Thesis Committee |
| _____ | _____ |
| Date | Dr. David McClenahan, Thesis Committee Member |
| _____ | _____ |
| Date | Dr. Nilda Rodriguez, Thesis Committee Member |
| _____ | _____ |
| Date | Dr. Michael J. Licari, Dean, Graduate College |

Dedicated to

Dr. Edward “Ned” Williams

TABLE OF CONTENTS

PAGE

# LIST OF TABLES

# LIST OF FIGURES

FIGURE PAGE

# CHAPTER 1

# INTRODUCTION AND LITERATURE REVIEW

## Neurulation

During early vertebrate development, the ectodermal germ layer becomes divided into three embryonic tissue components. The epidermis is the outermost tissue layer; it will surround the surface of the embryo and give rise to the skin. The neural tube and neural crest will form the majority of the nervous system. Cells of the neural tube differentiate into neurons and glial cells to form the central nervous system, whereas neural crest cells develop into the sensory neurons, autonomic neurons, and glial cells of the peripheral nervous system (Le Douarin 1982).

Neurulation is the formation of the neural tube and is a process undergone by vertebrate embryos early on in development. It is the basis of the entire adult central nervous system. This process is activated by the notochord, a flexible rod-shaped cellular structure that is found in all developing chordates and is derived from the mesoderm. The notochord serves as the foundation for the primordial axis of the embryo and a precursor for axial skeleton development (Lawson et al. 2001). Primary neurulation contains three major stages, including the formation of the neural plate, invagination of the neural plate and the advancement of the neural groove and neural folds, and is completed by the fusion of the neural folds forming a hollow tube, separating the roof of the neural tube and the overlying epithelium (Schoenwolf 1982). In chick embryos, this separation progresses caudally and terminates at somite pair 27 (Lawson et al. 2001).

Secondary neurulation is a process in which the caudal neural tube is formed through cavitation of the tail bud proceeding in the posterior direction from somite pair 28 (Schoenwolf 1991). In chicks, primary neurulation continues more dorsally while secondary neurulation occurs more ventrally creating a region of overlap. In this region the two neural tubes conjoin to form a single neural tube (Schoenwolf and Delongo 1980).

## Neural Crest Cells

Neural crest cells (NCCs) were first studied by the Swiss embryologist, Wilhelm His, in 1868. NCCs were identified in chick embryos as a population of cells that emanate from the crest of the neural tube, a region between the neural tube and ectoderm which later develops into the central nervous system (His 1868). NCCs are now described as multipotent neuroectodermal cells that originate between the neural tube and epidermis of vertebrates.

NCCs undergo an epithelial-to-mesenchymal transition (EMT), in which the cells disassemble and reorganize their actin cytoskeletons to become migratory. NCCs will migrate individually or in groups. Migratory NCCs follow distinct pathways directed by certain molecules associated with extracellular matrices, such as collagen, hyaluronic acid, and fibronectin. When NCCs reach their target destinations they begin to differentiate (Kirby and Hutson 2010). Ephrin ligands are also imperative for directing the migration pathways for many cell types during development. Transmembrane ephrins act as a bifunctional guidance cue by either blocking or stimulating the migration

of NCCs (Santiago and Erickson 2002). Ephrin-B proteins stimulate and guide the migration of NCCs destined to form melanoblasts along the dorsolateral pathway. However, early in development, ephrin-B proteins block the dorsolateral migration of NCCs before they are designated to migrate, preventing them from invading the pathways of other migratory cells and disrupting development. Ephrin-B proteins also repel NCC migration through posterior somite domains, thereby guiding them through the anterior domains only (Santiago and Erickson 2002).

Occludin is a protein associated with neurulation. As demonstrated experimentally in mice during the time the neural tube begins to close and EMT occurs, occludin is downregulated and causes tight junctions to become ineffective (Aaku-Saraste et al. 1996). As a result, the cadherin-based adherens junctions alter their configuration and distribution. This event allows the cells to disengage and become migratory. Stationary NCCs contain $Ca^{2+}$ adherens N-cadherin and cadherin-6B, but when EMT occurs they are downregulated (Revel and Brown 1976; Newgreen and Gooday 1985; Akitaya and Bronner-Frasier 1992; Nakagawa and Takeichi 1995; Nakagawa and Takeichi 1998). Cadherins associated with migration, such as cadherin-7 and cadherin-11, are upregulated and the NCCs become mobile (Tanihara et al. 1994; Hoffman and Balling 1995; Nakagawa and Takeichi 1998; Vallin et al.1998).

NCCs generate a variety of different structures in the developing embryo. They contribute to the dorsal root sensory ganglia and autonomic ganglia of the peripheral nervous system, and the aortic arch branches and aorticopulmonary septum of heart.

NCCs are also known to form craniofacial connective tissue, smooth muscle cells, skin melanocytes, the pituitary, cartilage, the bones that compose the floor of the skull and the middle ear, the connective tissues within the thymus, thyroid, and parathyroid (Le Douarin et al. 1993; Marsot-Dupuch et al. 2004; Shah et al. 1996).

NCCs also give rise to the ganglia of numerous cranial nerves. The nerves associated with the first, second, third and fourth pharyngeal arches are the facial (VII), glossopharyngeal (IX), vagus (X), and the trigeminal (V) with its three branches (ophthalmic, maxillary and mandibular) (Kirby et al. 1985).

In addition, NCCs play a pivotal role in the development of the eye. NCC derivatives include structures such as the iris, ciliary body, choroid, stroma of the cornea, sclera and portions of the extra-ocular muscles that control the movement of the eye (Creuzet et al. 2005).

As demonstrated experimentally through transplantation and cell cultures, extracellular signaling mechanisms can affect the fate of neural crest cells (Dorsky et al. 1998; Bronner-Fraser 1993; Stemple and Anderson 1993; Le Douarin et al. 1994). Growth factors have been proven to influence the migration, proliferation and differentiation of uncommitted neural crest cells. Experimentally, a deletion of the gene that codes for platelet-derived growth factors has been shown to result in mutant mice that display malformations of the cranial bones (Soriano 1997). It was also found that glial growth factor promotes glial differentiation of rat neural crest stem cells by suppressing neuronal differentiation, supporting the idea that growth factors may choose

the fate of some neural crest cells at the expense of others (Shah et al. 1994). Similarly, Wnt-1 and Wnt-3a are genes found to influence the fate of neural crest cells. These genes are expressed by medially located neural crest cells. In zebrafish, the Wnt signaling pathway and its role in neural crest cell fate was assessed by injecting cytoplasmic β-catenin messenger RNA into lateral neural crest cells before they became migratory. The injected cells were induced to form pigmented cells instead of neurons or glial cells (Dorsky et al. 1998).

## Cardiac Neural Crest Cells

Cardiac NCCs comprise a subpopulation of NCCs that originate in the posterior cranial region of the neural tube. Cardiac NCCs migrate bilaterally along the pharyngeal arches toward the cardiac outflow tract of the heart (Kirby et al. 1983; Poelmann and Gittenberger-de Groot 1999; Hutson and Kirby 2003, Kaartinen et al. 2004). Cardiac NCCs are responsible for forming the great vessels, cardiac ganglia, and the aorticopulmonary septum that divides the aortic and pulmonary trunks and separates the cardiac outflow tracts (review by Rosenquist 2013). Cardiac NCCs also responsible for shaping the pharyngeal arches and their derivatives, and they contribute to forming the walls of the proximal coronary arteries (Kirby and Waldo 1995; Poelmann et al. 1998; Poelmann and Gittenberger-de Groot 1999). Cardiac NCCs provide structure and guidance that is vital for normal cell development of the heart and great vessels. Congenital heart defects that model those observed in humans can be generated

experimentally through disturbing the cardiac NCC population in animals (Rosenquist and Finnell 2001).

It has been suggested that the migratory NCCs that enter the heart and reach their target destination will then stop differentiating and commit to an apoptotic pathway (Poelmann and Gittenberger-de Groot 1999). It is because of this well-regulated, programmatic cell death and change in the electrophysiological behavior of the heart that cardiac NCCs are believed to mediate the formation and separation of the cardiac conduction system and the surrounding myocardium (Poelmann and Gittenberger-de Groot 1999). It is also speculated that apoptotic cardiac NCCs are responsible for the separation of the outflow tract and the atrioventricular regions of the heart. Failure of the NCCs to undergo normal development and then enter apoptosis could result in cardiac outflow tract abnormalities and atrioventricular septal malformations in the heart, which are among the most frequently occuring abnormalities of all birth defects (Poelmann and Gittenberger-de Groot 1999).

## Neural Crest Cell Migration Pathways

Traditionally, the neural crest was divided into two major regions known as the cranial and neural crest (Kirby and Waldo 1990). The cranial neural crest is located in the area between the mid-diencephalon and the caudal limit of somite 5. The truck neural crest extends from somite 5 to the caudal end of the embryo (Kirby and Waldo 1990). However, in recent years it has become apparent that there is another population of neural

crest cells emanating posteriorly from the rhombencephalic region, commonly called the circumpharyngeal neural crest or cardiac neural crest (Carlson 2013).

The cardiac neural crest is a region within the cranial neural crest between the midotic placode and the caudal limit of somite 3. The neural crest cells that migrate into the cardiac outflow tract and form the aorticopulmonary septum are derived from the cardiac neural crest. The cells of the cardiac neural crest migrate from the neural fold and populate in pharyngeal arches 3, 4, and 6 (Miyagawa et al. 1990). While in the pharyngeal arches, the NCCS shape the endothelium of the aortic arch arteries (Bockmam et al. 1989). The NCCs from pharyngeal arch 4 are involved in the development of cardiac outflow septation (Thompson and Fitzharris 1979).

During the development of the anterior portion of the eye, successive waves of neural crest cells invade the area between the lens and the corneal epithelium. These mesenchymal NCCs contribute to the tissues that line anterior chamber, such as the cornea, the iris stroma, the anterior chamber angle and the trabecular meshwork (Hay 1980). In chick embryos, neural crest cells migrate toward the border of the optic cup by stage 18 (Bard and Hay 1975). Approximately 24 hours later, around stage 23, the first wave of NCCs, the cells closest to the lens, migrate between the lens and corneal epithelium. The NCCs form a simple cuboidal epithelium and separate the primary corneal stroma from the lens (Bard and Hay 1975). By stage 26, this layer develops into the corneal endothelium. At stage 27, another wave of NCCs migrate to the primary corneal stroma and take residence in the stroma where they later become the fibroblasts of the cornea (Fitch et al. 1998; Hay 1980).

In a study by Beebe and Coats in 2000, the relationship between the lens and NCCs was examined. Removal or replacement of lens led to formation of a disorganized mass of mesenchymal NCCs accumulating under the corneal epithelium. The tissues that are derived from NCCs were not found in the eyes missing their original lenses. When the lens was replaced shortly after removal, within 48 hours after surgery, the corneal endothelium and anterior chamber were formed beneath the lens. When only a portion of the lens was removed, the mesenchymal cells differentiated into corneal endothelium under the remaining part of the lens. Beebe and Coats (2000) discovered that the mesenchymal NCCs that come into contact with the anterior epithelial cells of the lens express the cell adhesion molecule N-cadherin, and can form an organized layer. These studies support the theory that the formation of the corneal endothelium is regulated by signals from the lens and the expression of N-cadherin. N-cadherin may be a key factor in the mesenchymal-to-epithelial transition that is necessary for NCCs to undergo prior to the formation of the corneal endothelium.

## Homocysteine

Congenital malformations, such as atypical development of the cardiac outflow tract, great vessels, and associated valves, can be due to abnormal proliferation, migration and differentiation of cardiac NCCs that occurs in the presence of elevated levels of maternal serum homocysteine (Hcys) (Kirby 1987).

Hcys is a sulfur-containing, non-essential amino acid found in the blood that acts as a metabolite in the formation of the essential amino acid, methionine (Miller 2003).

Hcys serves a fundamental role as an intermediate in the folic acid cycle, existing between S-adenosylmethionine, the methyl donor, and the synthesis of folic acid and vitamin B12 (Miller 2003). Hcys is either irreversibly degraded to cysteine via the transsulphuration pathway or it requires folate to be remethylated and converted back to methionine (review by Blom and Smulders 2011, review by Rosenquist 2013).

In 1969, Kilmer McCully observed vascular lesions in two patients suffering from severe hyperhomocysteinemia due to separate complications of homocysteine metabolism (McCully 1969). McCully proposed the "homocysteine theory," which stated that elevated plasma concentrations of Hcys, or a derivative of Hcys, yield potentially detrimental effects on the vascular wall. Later studies have confirmed that there is a well established link between elevated plasma homocysteine concentrations and the risk of developing cardiovascular diseases (reviewed by Blom and Smulders 2011; Miller 2003).

The teratogenic effects of Hcys are due to its ability to alter the cytoskeleton of NCCs, thus changing the cells' normal differentiation and migration. The findings in a study done by Boot et al. in 2003 gave evidence that elevated Hcys is involved with enhancing the EMT of NCCs. Neural tube explants treated with folic acid were found to have increased NCC differentiation into nerve and smooth muscle cells, while the neural tube explants treated with Hcys exhibited increased migration and outgrowth and reduced differentiation of NCCs. These results suggest that neural tube, orofacial and conotrucal defects can be explained by abnormal behavior of NCCs exposed to

hyperhomocysteinemia and the critical role folic acid plays in NCC differentiation and migration (Boot et al. 2003).

It is known that adequate intake of folic acid through diet and/or dietary supplements throughout a pregnancy can significantly lower the risk of congenital embryonic neural tube and cardiovascular malformations (Milinsky et al. 1989). Although the protective effects of folic acid during embryonic development are not entirely understood, it is established that that homocysteine metabolism is involved in the underlying mechanism.

In a study done by Rosenquist et al., in 1996, varying concentrations of Hcys, comparable to those found in humans, were administered to avian embryos and a dose response was established. Of the embryos treated with a teratogenic dose of 200 mM D,L-homocysteine or 100 mM L-homocysteine thiolactone during days 0, 1 and 2 of incubation, 27% showed neural tube defects. Embryos were also exposed to teratogenic doses during incubation days of 2, 3 and 4 to determine the effects of Hcys on the septation process of the heart. Ventricular septal defects were apparent in 23% of the surviving embryos, while 11% showed neural tube defects. However, the embryos that were administered a supplementary daily dose of 0.1 mg (100.0 ng) of folic acid following the doses of Hcys were spared of the teratogenic effects (Rosenquist et al. 1996).

## Folic Acid Cycle

A review by Rosenquist, (2013) explains folate as a collective term used to describe a collaborative set of compounds and intermediates that have similar metabolic activities in the folate cycle. Folate enters the cycle by binding to folate receptors on the surfaces of cells (review by Minoux and Rijli 2010). Folic acid is a general term coined to describe the synthetic form of water-soluble B-vitamin folate. Dietary supplemental folates are the most stable form of folates. Folates exist predominantly as polyglutamates, which must be hydrolyzed to monoglutamates in order to be transported into the cycle (review by Minoux and Rijli 2010). Rapidly dividing cells, such as cardiac neural crest cells, express a high-affinity folate receptor on their surface (review by Rosenquist 2013). Folate is converted into tetrahydrofolate (THF) and then to 5,10-methylene-THF by action of enzyme serine hydroxymethyltransferase (SHMT) (review by Minoux and Rijli 2010). This conversion supplies the methyl groups needed for nucleotide synthesis in cell division (Wagner 1995). The enzyme 5,10-methylenetetrahydrofolcate reductase (MTHFR) reduces 5,10-methylene-THF to 5-methyl-THF (Wagner 1995). The methyl group of 5-methyl-THF is then used to transfer Hcys into the S-adenosylmethionine (SAM) Cycle to regenerate methionine from Hcys by the enzyme methionine synthetase and coenzyme vitamin B12 (Wagner 1995). The SAM Cycle uses coenzyme Vitamin B6, enzyme cystathionine beta-synthase ultimately, and intermediates SAM and S-adenosylhomocysteine to convert Hcys into methionine and release cystathionine (reviewed by Rosenquist 2013).

Insufficient levels of folate, faulty folate receptors, or inhibition of folate receptor expression may each or in combination result in a reduced availability of THF, which then causes fewer methyl groups to be used for DNA synthesis in cells such as cardiac NCCs (reviewed by Rosenquist 2013). Deficiencies or mutations of any of the key enzymes used in the cycles may lead to elevated levels of Hcys, which has been experimentally connected to neural tube defects (NTD) and congenital heart defects (CHD) (reviewed by Rosenquist 2013).

## Congenital Heart Defects

Congenital heart defects (CHDs) are the most common developmental abnormality in newborns and are the leading non-infectious cause of mortality (Garg et al. 2003). In the United States, out of every 1,000 live births approximately 8 to 10 babies are affected by a CHD (Botto et al. 2003). Less than 15% of heart defects can be determined from a known cause (review by Minoux and Rijli 2010). Congenital heart defects can be attributed to exposures to environmental effects, maternal factors and genetic disposition (Shaw et al. 2001, Botto et al. 2003). According to a study by Hobbs et al. (2010), women with functional polymorphisms in genes responsible for encoding the function of folate metabolism pathways increase the risk of carrying a fetus with CHD when maternal lifestyle factors such as obesity, smoking, and/or drinking alcohol are present. Several studies have shown a correlation between the development of neural tube and CHDs in embryos exposed to increased maternal plasma homocysteine present in conditions of folate depletion. Folate deficiency can lead to CHDs, neural tube defects

(NTDs), recurrent early pregnancy loss, late pregnancy complications, and orofacial clefts (review by Minoux and Rijli 2010). Elevated maternal homocysteine is also associated with neurodegenerative and psychiatric disorders, osteoporosis and cancer (see reviews by Rosenquist 2013; Hobbs et al. 2005; Minoux and Rijli 2010).

It is characteristic of successful NCCs to rapidly divide and proliferate because they have a higher mitotic index compared to neighboring embryonic cells in the neural tube region (Salvarezza and Rovasio 1997; Tierney et al. 2004; Rosenquist et al. 2010). NCCs and cardiac NCCs must begin to enter the S-phase of mitosis before they can initiate EMT (Burstyn-Cohen and Kalcheim 2002; Tierney et al. 2004). As reviewed by Rosenquist (2013), folate is used as a transportation system for methyl groups in the SAM cycle and has a vital role in nucleotide synthesis, therefore a deficiency in folate will block this key step in cell division and impair NCC proliferation and migration.

Early in development, demethylated maternal and paternal genes undergo a widespread re-methylation that occurs in a predetermined, coordinated sequence associated with differentiation (reviewed by Rosenquist 2013). Enzymes DNA (cytosine-5)-methyltransferase 3a (DNMT3a) and DNMT3b control the fate and migration of NCCs during this time of re-methylation (reviewed by Martins-Taylor et al. 2012). Demonstrated experimentally by Martins-Taylor, et al. (2012), when folate is depleted the expression of DNMT3b is inhibited and the re-methylation of DNA is reduced. As a result, the genes needed for the sequenced regulation of NCCs are not silenced in an orderly manner, causing several genes to be abnormally expressed or over-expressed. These findings support the hypotheses that a folate deficiency could play a pivotal role in

decreased DNA methylation causing CHDs due to abnormal development of cardiac neural crest, and that folate supplementation may have a protective effect by rejuvenating DNA methylation (reviewed by Rosenquist 2013).

The majority of congenital heart defects (CHD) are due to abnormal development of the cardiac outflow tracts. The development of the cardiac outflow tracts is dependent on normal migration and differentiation of Cardiac NCCs.

## LIM3 Protein

The LIM domain is a particular cysteine-rich polypeptide sequence motif that creates a double zinc finger structure with a conserved consensus sequence of ($CXXCX_{16–23}HXXCXXCXXCX_{16–21}CXX(D/H/C)$). This domain is found in proteins that act as transcription factors or as components of focal adhesions or the actin-based cytoskeleton (Nishiya et al. 1999). Transcription factors (TFs) have essential roles in the foundation, structure and maintenance of cellular phenotypes (Edqvist et al. 2009).

Proteins containing LIM domains often have other domains, including homeodomain, kinase, SH3, and LD domains. The association of the tyrosine-based motif of the insulin receptor with the LIM 3 domain of the Enigma protein is a commonly described LIM domain mediated interaction. Likewise, the LIM 2 of Enigma interacts with the Ret receptor tyrosine kinase. These interactions demonstrate that each individual LIM domain needs to recognize and interact with other specific protein domains. For example, LIM 3 domain of paxillin, a signal transduction adaptor protein, is essential for the targeting of focal adhesions (Côté et al. 1999).

In a study conducted by Rosenquist et al. (2007), microarray analysis and expression profiling was performed on chick embryos to identify 65 transcripts of genes of known function that were altered by Hcys. The genes involved in cellular migration and adhesion were greatly affected. LIM3 (also known as cysteine and glycine rich protein 3, CPR3) mRNA was found to have increased to 176 times greater in the Hcys treated cells than in the controls. LIM3 protein participates in the complex control of the dynamic process of assembling and organizing the cell's actin cytoskeleton during EMT of the NCCs. LIM3 protein works as a transcriptional factor for the differentiation of motor neurons and interneurons (Khurana et al. 2002). LIM3 has a potential role in transcriptional regulation of certain genes during morphogenesis of the pituitary and pineal gland (Khurana et al. 2002). LIM3 has been found in nuclei, focal adhesions, and in the cytoplasm of NCCs (Khurana et al. 2002).

## Hypothesis

Mwakikunga et al. (2011) found that levels of LIM3 around nuclei and in focal adhesion of migrating chick embryo NCCs was enhanced in the presence of Hcys in vitro, suggesting that it may be involved in modulating the signal that adjusts the cytoskeleton for the enhanced migration. And given that Boot et al. (2003), have shown that Hcys enhances EMT, it may be that Hcys causes an upregulation of LIM3, which could be present in at least some cardiac NCCs, and if upregulated, may be responsible for enhanced (or otherwise altered) migration leading to malformations. In this study, the expression of LIM3 in migrating cardiac NCCs will be analyzed using confocal

fluorescence microscopy in conjunction with the marker antibody HNK-1 for NCCs to determine whether these NCCs (and others nearby) do show enhanced LIM3 expression.

# CHAPTER 2

# MATERIALS AND METHODS

## Culture and Fixation

Chicken eggs of the crossed strains Black Astrolorps/New Hampshire Red were purchased from Sunray Hatchery, Hazelton, IA. The eggs were incubated at 38˚C for 48 hours. The embryos were found to be between stages 11 to 14 (Hamburger and Hamilton 1992). The eggs were windowed after removing 4 mL of ovalbumin using a 20 gauge needle and syringe. Strips of Scotch tape were placed over one half of the egg covering the puncture hole, and a portion of the shell was removed by cutting a large oval window through the shell and the tape. To treat embryos, they were injected with 1µl of 100 µM Hcys into their amnions at the level of the 4$^{th}$ somite pair, under the developing heart. Control embryos were injected with 1 µl of Earl's Balanced Salt Solution (EBSS) in the same area. The windows were closed with Scotch tape and the embryos returned to incubate at 38˚C with high humidity. After 24 hours, the embryos were removed using 3MM filter paper rings and were rinsed in sterile plastic dishes with Chick Ringer's saline. The embryos were fixed by transferring to ice-cold 20% DMSO in methanol for 1 hour.

## Dehydration, Embedment and Sectioning

After fixation embryos were washed three times, two minutes each in phosphate buffered saline (PBS) (4% NaCl, 0.1% KCl, 0.1% KH2PO4, 0.575% NaHPO4, pH 7.4).

The embryos were dehydrated in a series of six ethanol solutions, including 25%, 50%, 70%, 90%, and twice in 100% for five minutes each. The embryos were then incubated in a 1:1 mixture of Protocol Safeclear II (Fisher Scientific, Chicago, IL) and ethanol for fifteen minutes, and then 100% Protocol Safeclear II for ten minutes at room temperature followed by ten minutes at 60˚C. The embryos were then transferred to 1:1 paraffin and Protocol Safeclear II overnight at 60˚C, and then to 100% paraffin for an overnight incubation at 60˚C. The explants were finally transferred to fresh 100% paraffin and allowed to cool. They were mounted on wooden blocks and the paraffin was trimmed into a trapezoid blockface over the embryo. They were sectioned into six µm thick slices using a Reichert-Jung Histocut 820 microtome. The sections were floated on water at 42-45˚C on glass slides prepared with tissue section adhesive. The sections were allowed to dry and adhere on to the slides overnight. The slides were submerged for five minutes each in Coplin jars containing 100% Xylene (2x), 1:1 Xylene and 100% ethanol twice, 100% ethanol, 95% ethanol, 70% ethanol, 50% ethanol, deionized H2O twice, and then PBS.

## Immunohistochemistry

The sections were incubated in blocking solution (0.5% bovine serum albumin, 1% Tween-20, and 1% non-fat dry milk in PBS) for ten minutes at room temperature. Monoclonal anti-LIM3 antibody purchased from the Developmental Studies Hybridoma Bank was diluted 1:100 in blocking solution and applied to the sections for two hours at room temperature or 24 hours at 4˚C. Primary antibody incubation was then followed by

three PBS washes for five minutes each. The binding of the anti-LIM3 antibody was detected using Alexaflour 488 tagged anti-mouse IgG (2 mg/Ml, Molecular Probes, Inc., Eugene, OR) diluted 1:500 in blocking solution for two hours at room temperature or 24 hours at 4˚C. The secondary antibody incubation was followed by three PBS washes for five minutes each. HNK-1 primary antibody (American Type Culture Collection, Manassas, VA), obtained from hybridoma cell cultures was used to detect neural crest cells. It was diluted 1:100 in blocking solution and applied to the slides for two hours at room temperature for 24 hours at 4˚C. The HNK-1 primary antibody was a gift from Dr. Alicia Paulson at the University of South Dakota. This was followed by three PBS washes for five minutes each. To detect the HNK-1 primary antibody, the slides were incubated in Alexafluor 594 tagged anti-mouse IgM with minimal cross-reactivity to human, bovine, and horse (1.4mg/ml, Jackson ImmunoResearch Laboratories Inc, West Grove, PA) diluted 1:500 in blocking solution for two hours at room temperature or 24 hours at 4˚C. This was followed by three PBS washes for five minutes each. To stain the nuclei of the cells, the slides were incubated in 1µg/ml bisbenzamide (Hoescht No. 33258 Sigma Chemical Co, St. Louis, MI) for ten minutes in the dark at room temperature, then rinsed in deionized water for 10 seconds. Two to three drops of Dapi Fluoromount-G anti-fade mounting medium (Southern Biotech, Birmingham, AL) was added to each slide. The slides were then covered with microscope cover glass (22x50-1.5, Fisher Scientific), and allowed to dry.

## Image Analysis and Microscopy

The slides were viewed using a Zeiss LSM 510 confocal microscope and Zen 2011 software for each of the two fluorescent labels. Images were captured with excitation and emission wavelengths chosen by the software after adjusting the pinhole and laser intensities. The fluorescence intensity of LIM-3 immunostaining was measured using the 2-D option, dragging the cursor over each cell and recording the intensity value that was given on a scale of 0-255. Background reference intensity was measured by determining the average brightness values of 20 points on the neural tube in the same image. The values of the neural crest cell brightness were divided by the average background brightness to obtain a fluorescence ratio.

# CHAPTER 3

# RESULTS

Chick embryos were incubated to the stages of 11-14. The treated chick embryos were injected with 1µl of 100 µM Hcys into their amnions. The control embryos were injected with 1 µl of Earl's Balanced Salt Solution. The embryos were dehydrated, embedded in paraffin, and sectioned into 6 µm thick slices. The sections were labeled with monoclonal anti-LIM3 primary antibody, Alexafluor 488 secondary antibody, HKN-1 primary antibody and Alexafluor 594 secondary antibody. The sections were examined under Zeiss confocal microscope and intensity analysis was done using Zen 2011 software. During the course of this study 16 control embryos and 15 treated embryos were analyzed for LIM3 expression.

Neural crest cells are known to migrate and contribute to the development of tissues and structures in the heart, the eye and around the axial skeleton. These three areas were chosen for this study. The results are divided into findings for each of the tissue types.

## Paraxial Mesenchyme

The LIM3 stained cells observed in the mesenchyme around the neural tube in Hcys treated embryos exhibited higher intensity staining of Alexafluor 488 compared to the LIM3 positive cells seen in control embryos. The number of LIM3 positive cells existing in the control and treated specimens is comparable. As seen in Figure 1A and

1B, the intensity of the stained cells is bright compared to the background staining in the mesenchyme, however, in Hcys-treated embryos the intensity was consistently much higher. Whereas, Figures 1C and 1D exhibit a low level of background staining and highly intense staining of LIM3 positive cells.

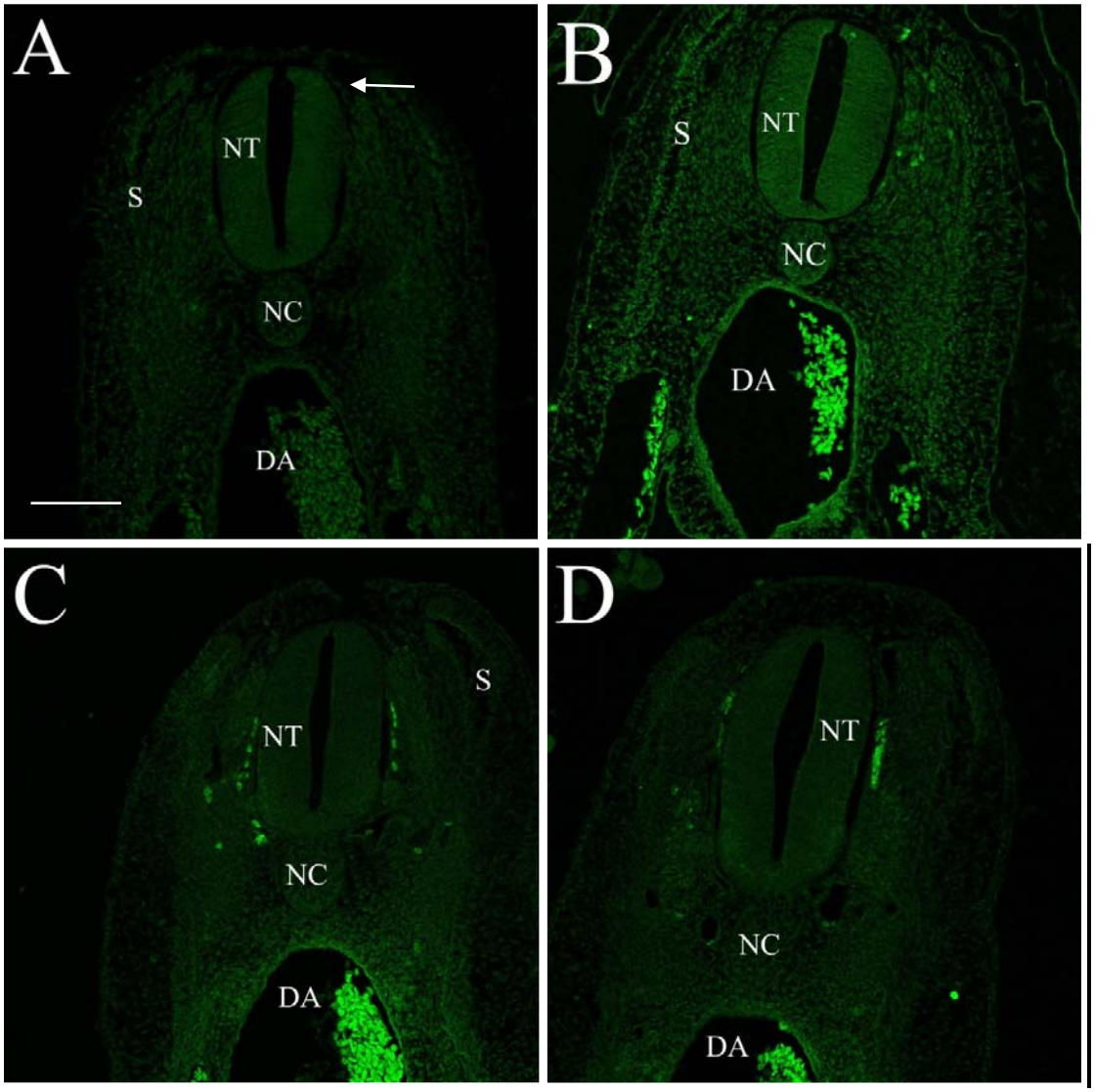


(Figure Continues)

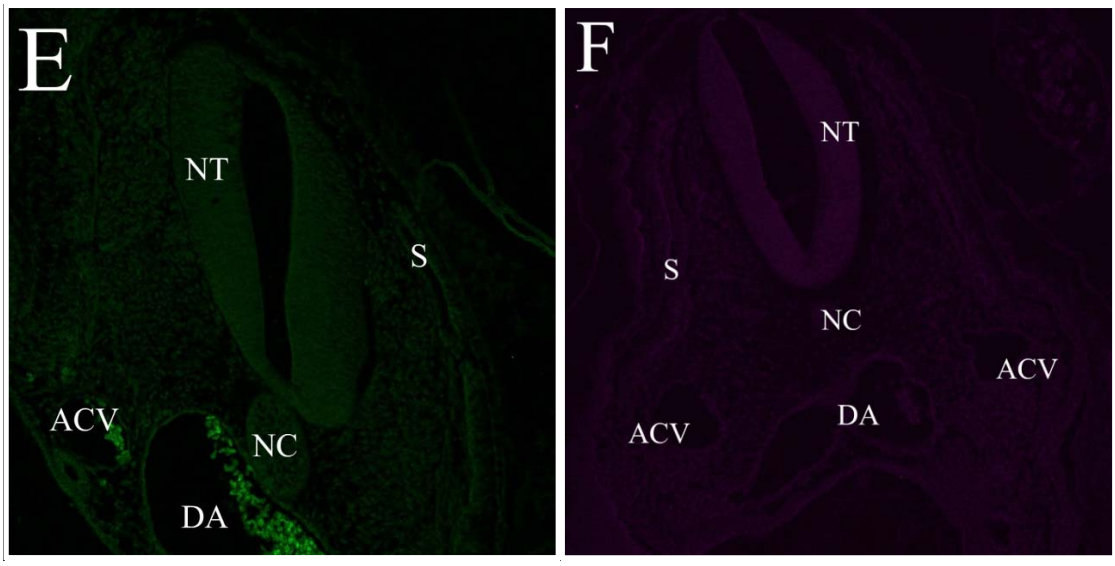


Figure 1. Sections through the trunk of HH stage 11-14 embryos stained with anti-LIM3 protein revealing paraxial mesenchyme with migratory cells. LIM3 is shown with green fluorescence and HNK-1 is shown with magenta fluorescence. A and B. Control embryo sections showing LIM3 positive cells present in the paraxial mesenchyme. Note that background fluorescence varied with section thickness (and possibly other factors) and is very low in A, higher in B. Red blood cells in the descending aorta show strong autofluorescence. C and D. Similar sections through Hcys treated embryos. Background fluorescence is similar to that in A. Fluorescence of scattered LIM3-positive migratory cells is considerably more intense. E and F. Negative control embryos. E is a negative control for anti-LIM3 primary antibody. F is a negative control for HNK-1 primary antibody. NT= Neural Tube; NC= Notochord; S= Somite; DA= Descending Aorta; Scale Bar= 100 μm.

The intensity of positively stained cells was measured using the confocal microscope image analysis software. The numerical intensity of each cell on a scale of 0 to 255 was converted to a ratio by dividing it by the average intensity measured in the neural tube in order to control for section thickness and other factors that might cause section-to-section variability. These ratios were recorded and analyzed statistically. A histogram plotting their frequency distribution is displayed in Figure 2. The ratios were

found to be not normally distributed but skewed with greater numbers of ratios having lower intensity. It was apparent that the ratios were more intense over the entire frequency distribution in Hcys-treated embryo sections. Box plots (Figure 3) showing medians, quartiles, maxima and minima reveal the magnitude of this difference. Because the data was not normally distributed it was compared using the Wilcoxon rank sum test. The difference in the paraxial region was highly significant.

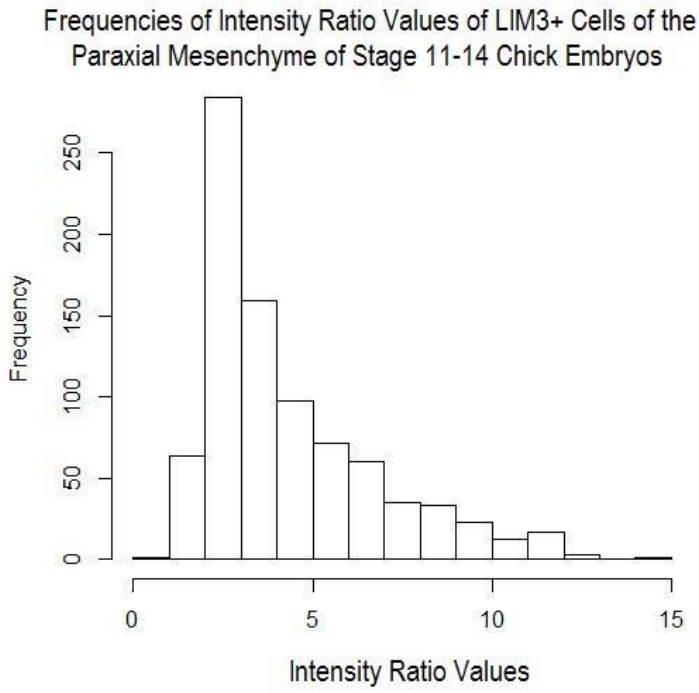


Figure 2. A histogram depicting the frequencies of the intensity ratio values of LIM3 positive cells observed in the paraxial mesenchyme of stage 11-14 chick embryos treated with 1µl of 100 µM Hcys or 1 µl of EBSS.

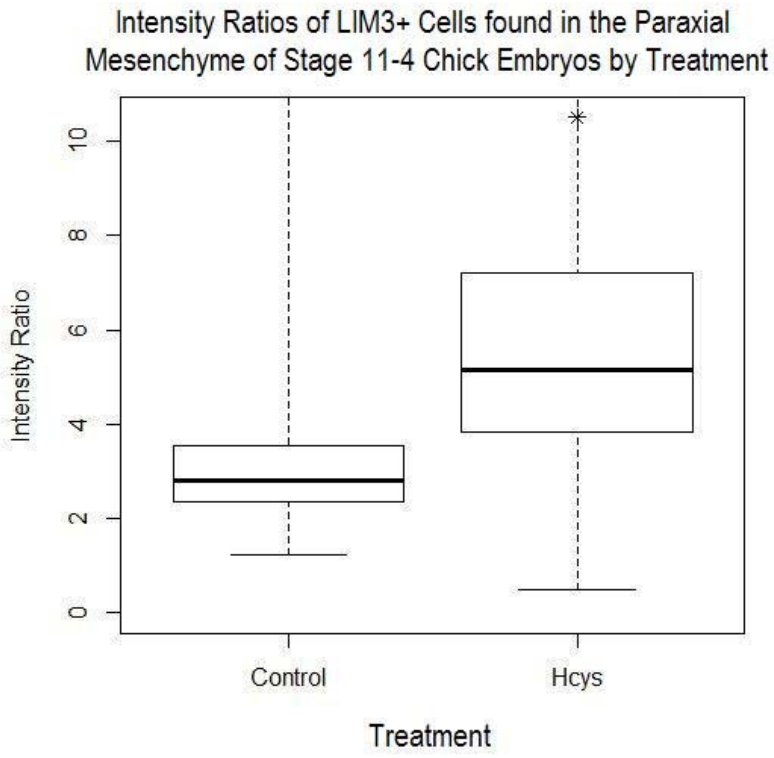


Figure 3. Box plots depicting the intensity ratio of LIM3 positive cells observed in the paraxial mesenchyme of stage 11-14 chick embryos treated with 1µl of 100 µM Hcys or 1 µl of EBSS (control). The heavy line in the box indicates median, the top and bottom lines of the box indicate third and first quartiles, respectively, and the whiskers connected to the box by dotted lines show maximum and minimum.
*Significantly different, P< 2.2e-16

## Periocular Mesenchyme

The mesenchymal tissue surrounding the early developing eye is also an important site where NCCs must migrate in and eventually form the corneal endothelium and other structures. The number of LIM3 positive cells entering the periocular mesenchyme was similar in the control and treated embryos. As seen in Figure 4C and D, the stained cells of the treated embryos exhibited a greater intensity of staining

compared to the intensity of the stained cells seen in the control group (A and B). The pattern observed around the ocular mesenchyme was similar to that of the paraxial mesenchyme. Although the intensity of stained cells was generally quite intense in controls, higher overall than in the paraxial mesenchyme, it was clearly augmented in Hcys-treated embryos.

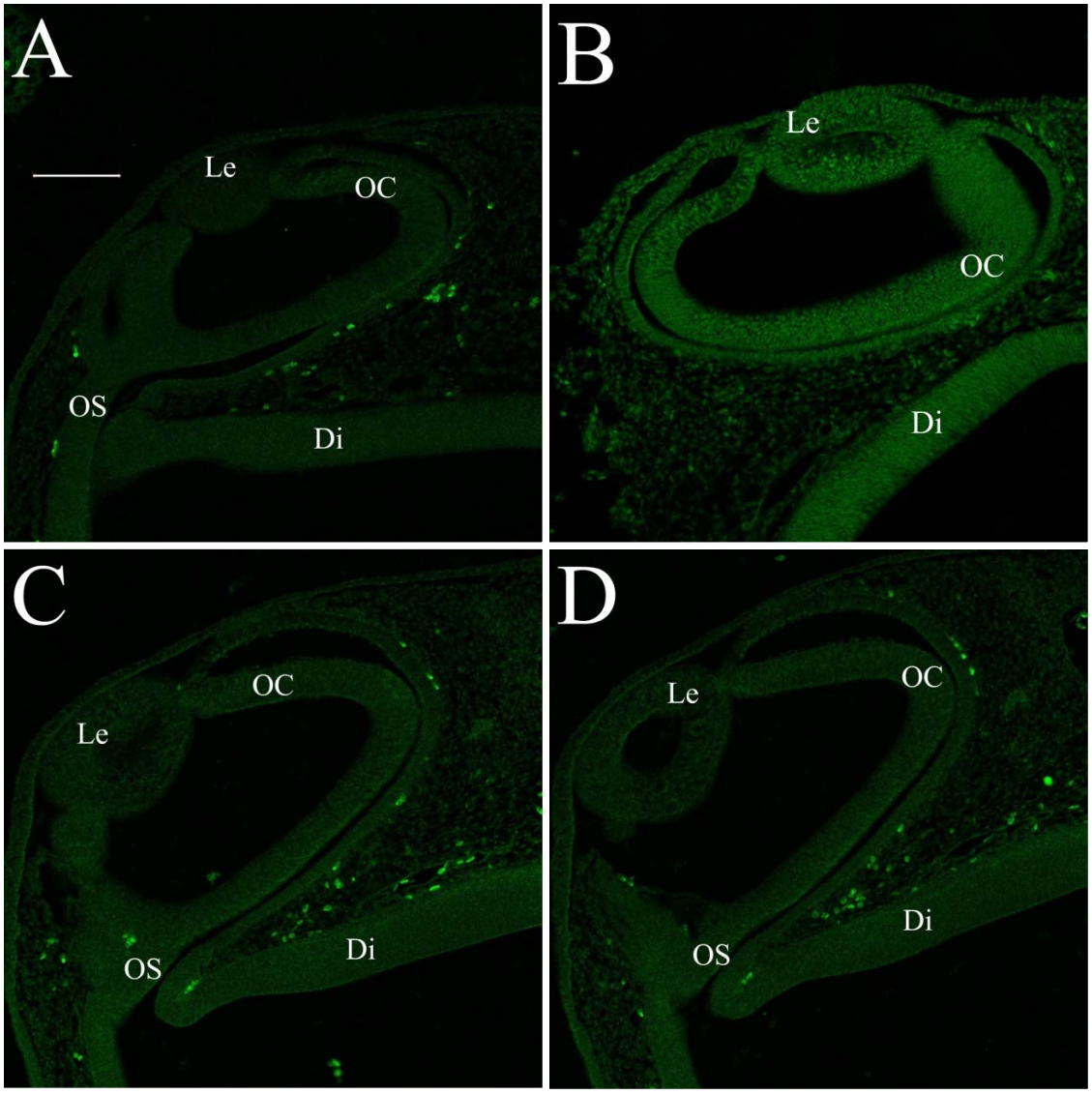


Figure 4. Sections revealing LIM3-positive cells in the periocular mesenchyme around the optic cup. A and B. Control embryo sections at low (A) and higher background intensity (B) likely due to section thickness. LIM3 stained cells are scattered and clearly visible. Some are quite near the sensory retina. C and D. Hcys-treated embryo sections of moderate and similar background fluorescence. Stained cells are intense. Le= Lens; OC= Optic Cup; OS= Optic Stalk; Di= Diencephalon; Line= 100 μm.

The intensity ratio data associated with the periocular mesenchyme, as with the paraxial mesenchyme, was not found to be normally distributed. The data are shown in Figure 5.

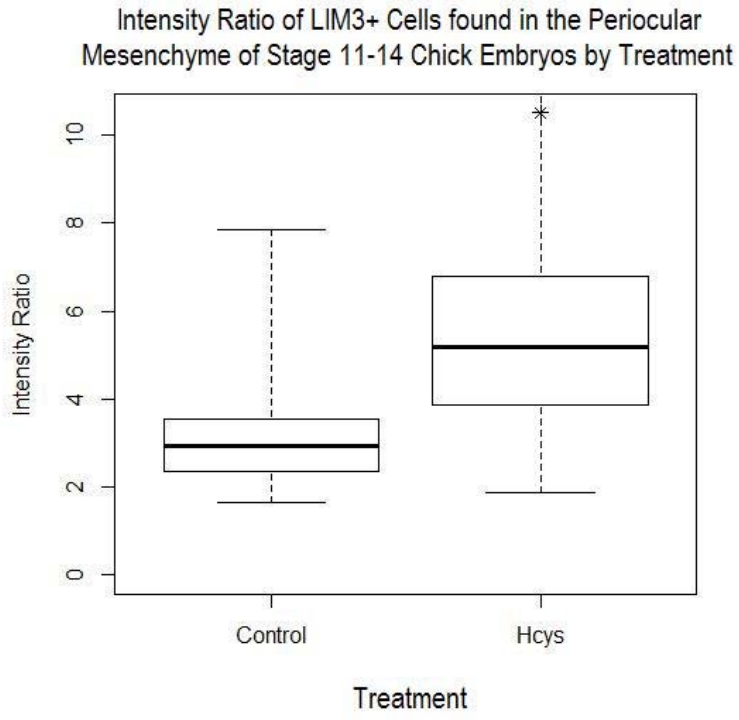


Figure 5. A box plots depicting the intensity ratio of LIM3 positive cells observed in the periocular mesenchyme of stage 11-14 chick embryos treated with 1µl of 100 µM Hcys or 1 µl of EBSS (control). Heavy lines indicate medians, top and bottom lines third and first quartiles, and whiskers show maximum and minimum.
*Significantly higher than control, $P < 2.2e-16$, Wilcoxon rank sum test.

## Pharynx Region

NCCs migrate from the neural tube region between rhombomeres 6 and 8 to the third somite in a ventral direction and enter the regions around pharyngeal arches 3, 4,

and 6 (Sato and Yost 2003). Some NCCs migrate even further towards the heart and into the outflow tracts where they participate in forming the aorticopulmonary and truncal septa (Sato and Yost 2003). These are known as cardiac neural crest cells. We found fewer NCCs in the pharynx region of both control and treated embryos than we found in the periaxial and periocular regions. This may be due to the fact that the chick embryos were only allowed to develop to HH stage 12-14 and the majority of neural crest cells do not reach this pathway until after the development of the pharyngeal arches, which occurs after HH stage 14 (Bellairs and Osmond 2005). Of the LIM3 positive cells that were observed in the pharynx region, the intensity ratios were stronger in the treated embryos in comparison to the control embryos.

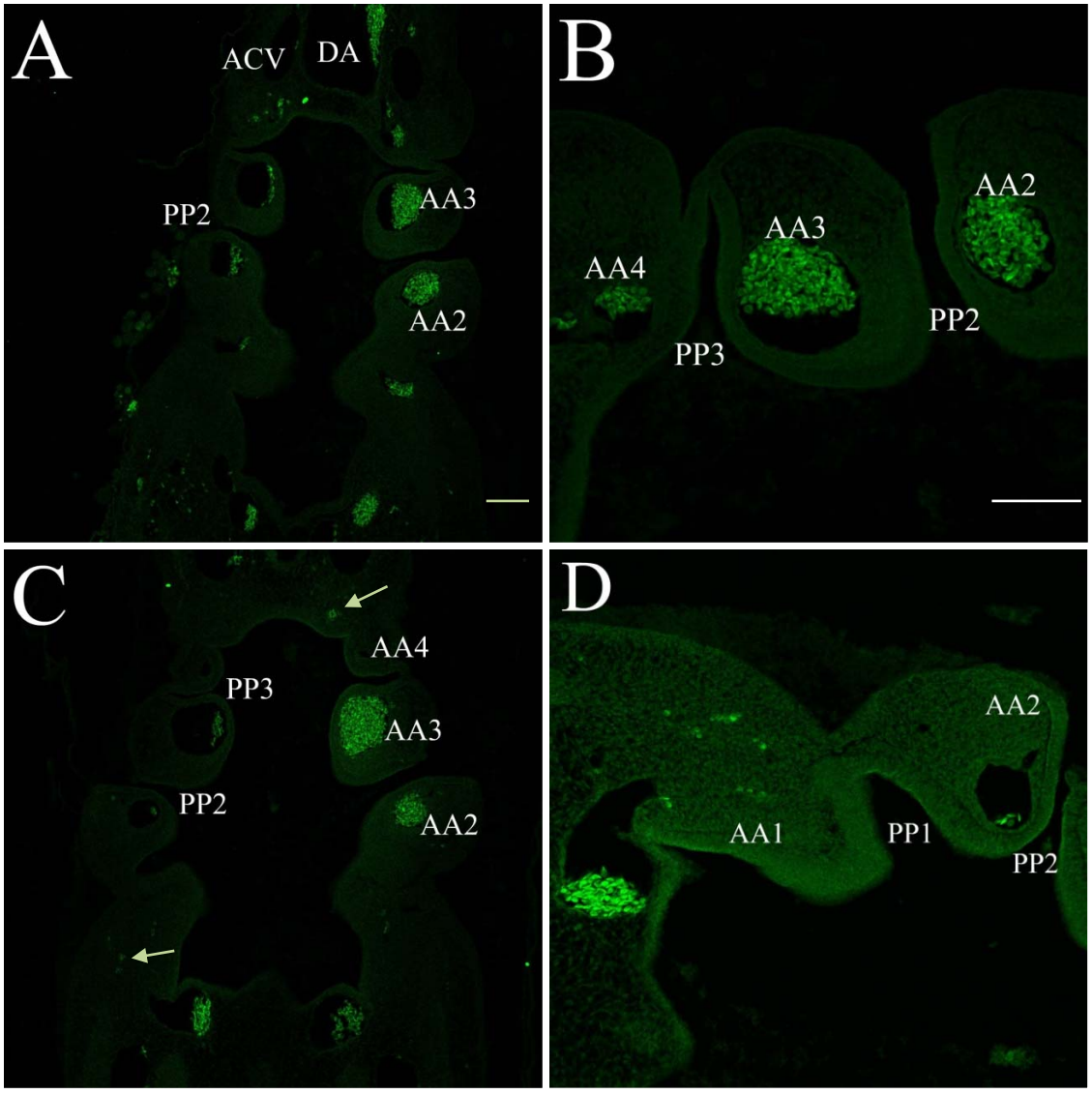


Figure 6. Sections through the pharynx region of HH stage 11-14 embryos stained with monoclonal anti-LIM3 primary antibody and Alexafluor 488 secondary antibody. A and B. Control embryos at low (A) and higher (B) magnification. C and D. Embryos treated with homocysteine. Autofluorescence of blood within the aortic arches is evident. LIM3-positive cells were scarce in both control and treated embryo sections. DA= Descending Aorta; ACV= Anterior Cardinal Vein; AA1= 1st Aortic Arch; AA2= 2nd Aortic Arch; AA3= 3rd Aortic Arch; AA4= 4th Aortic Arch; PP1= 1st Pharyngeal Pouch; PP2= 2nd Pharyngeal Pouch; PP3= 3rd Pharyngeal Pouch; Scale Bars= 100 µm; Arrows indicate possible LIM3 positive NCCs.

The intensity ratio data associated with the LIM3 positive cells found in the pharynx region was also not normally distributed. Box plots display the intensity ratios (Figure 7) of cells found in the pharynx region. The LIM3-positive cells in the Hcys treated group showed significantly greater intensity ratios than those of the control group.

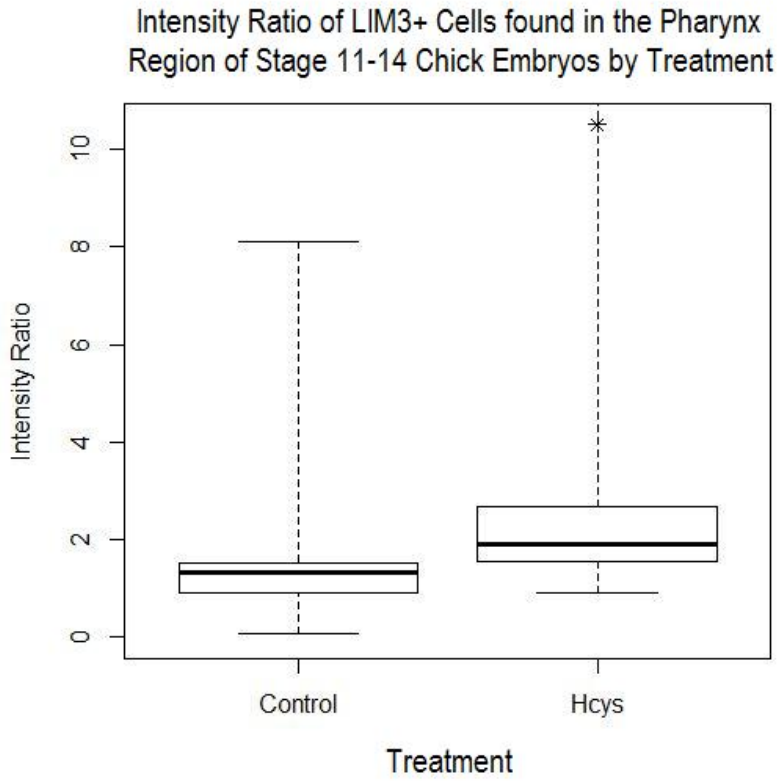


Figure 7. Box plots depicting the intensity ratio of LIM3 positive cells observed in the pharynx region of stage 11-14 chick embryos treated with 1µl of 100 µM Hcys or 1 µl of EBSS (control).
*Significantly greater than control, $P < 0.000001$.

## Wilcoxon Rank Sum Test and P-Values

Because the fluorescence intensity ratio was not normally distributed, it was assessed using the nonparametric Wilcoxon Rank Sum test. The results are shown in Table 1. The p-values associated with the Wilcoxon test confirm that the intensity ratios of the treated embryos are significantly different when compared to the ratios of the control group.

Table 1. The Results of the Wilcoxon Rank Sum Test with P-Values

| Location | Wilcoxon Sum | P-Value |
|---|---|---|
| Pharynx Region | 11046 | < 2.2e-16 |
| Paraxial Mesenchyme | 31281 | < 2.2e-16 |
| Periocular Mesenchyme | 3629.5 | < 2.2e-16 |

## Double Staining

Double staining with the antibodies to LIM3 and to NCCs (HNK-1) allowed us to identify cells that can be recognized as NCCs expressing LIM3 and to determine how many cells were NCCs not expressing LIM3 and how many cells expressed LIM3 but were not NCCs. Furthermore, it would allow us to determine whether Hcys treatment had any effect on the proportions of expressing cells. The majority of LIM3 stained cells did not display double staining with HNK-1. Approximately 27% of stained cells located in the paraxial mesenchyme were labeled by both Alexafluor 488 and Alexafluor 594. Of the neural crest cells in the periocular mesenchyme, 26% of the stained cells exhibited double staining. Only about 12% cells in the pharynx region were double stained. The percentage of double stained cells found in the paraxial mesenchyme, periocular

mesenchyme and pharynx region are listed by treatment in Table 2. The proportion of NCCs expressing LIM3 and HNK-1was lower than we expected and it may be that more NCCs come to express LIM3 later in their migration or developmental progress. Treatment with Hcys did not appear to alter the percentage of cells that double stained.

Table 2. Percent of NCCs expressing LIM3 by Location and Treatment

| Region | Treatment | Percent of NCCs expressing LIM3 |
|---|---|---|
| Pharynx Region | Control | 31/223 (14%) |
| Pharynx Region | Hcys | 22/189 (13%) |
| Paraxial Mesenchyme | Control | 22/189 (28%) |
| Paraxial Mesenchyme | Hcys | 56/236 (27%) |
| Periocular Mesenchyme | Control | 56/236 (23%) |
| Periocular Mesenchyme | Hcys | 64/216 (30%) |

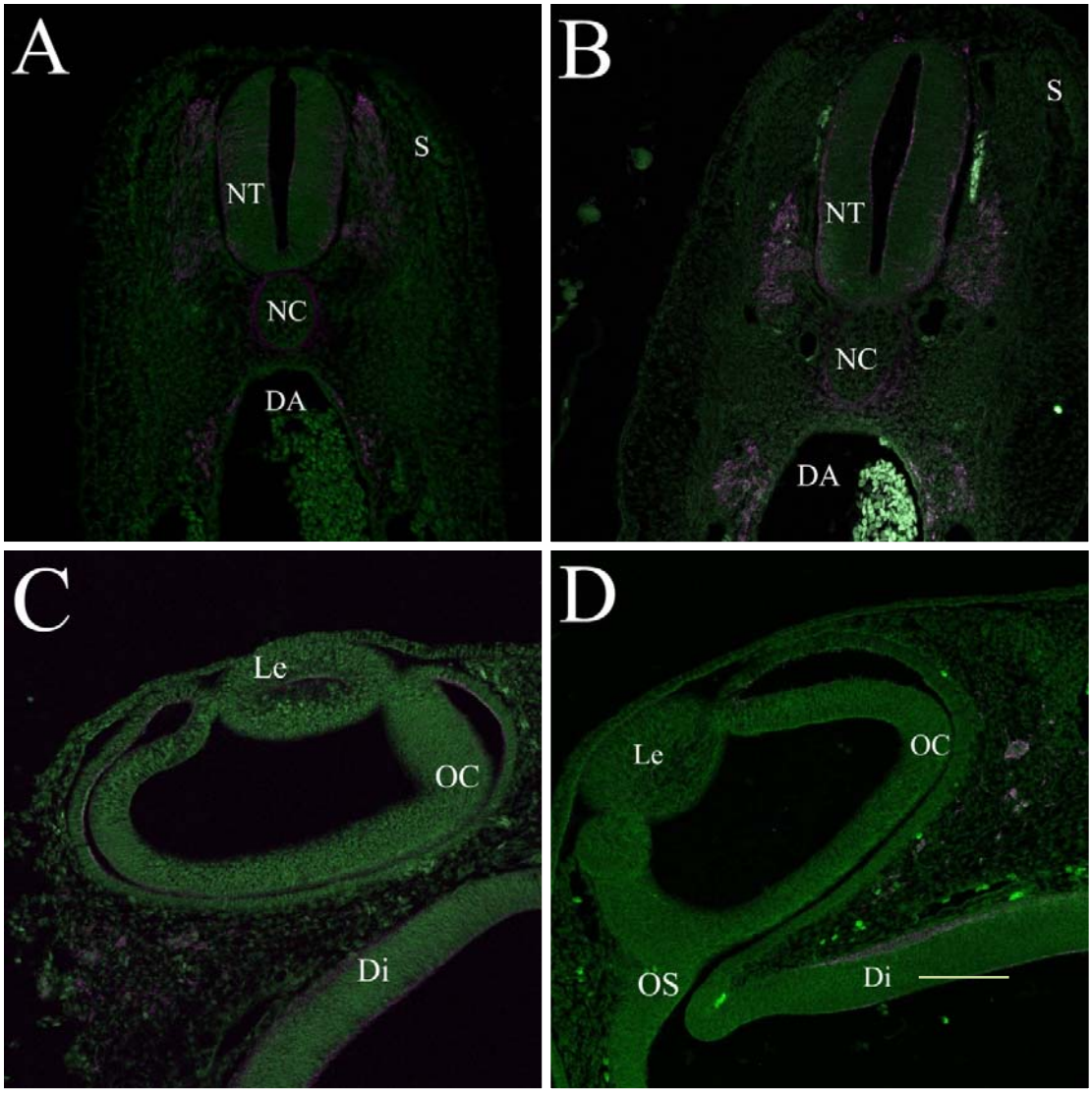


(Figure Continues)

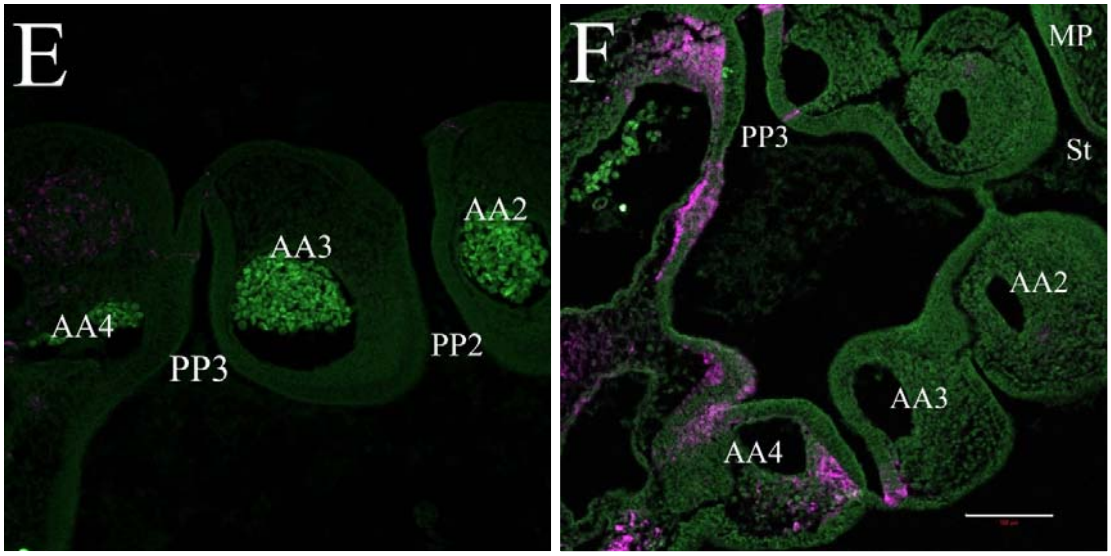


Figure 8. Sections through the trunk, optic cup and pharynx of HH stage 11-14 embryos labeled with monoclonal anti-LIM3 primary antibody, Alexafluor 488 secondary antibody, HKN-1 primary antibody and Alexafluor 594 secondary antibody. The light gray or white portions signify a cell that expresses LIM3 protein and is a possible neural crest cell. (A) is the neural tube of a control embryo. (B) the neural tube of a homocysteine treated embryo. (C) is the periocular mesenchyme region of a control embryo. (D) is the periocular mesenchyme region of a homocysteine treated embryo. (E) is the pharynx region of a control embryo. (F) the pharynx region of a homocysteine treated embryo. NT= Neural Tube; NC= Notochord; DA= Descending Aorta; S= Somite; OC=Optic Cup; OS= Optic Stalk; Di= Diencephalon; Le= Lens; AA2= 2$^{nd}$ Aortic Arch; AA3= 3$^{rd}$ Aortic Arch; AA4= 4$^{th}$ Aortic Arch; PP2= 2$^{nd}$ Pharyngeal Pouch; MP= Mandibular Process; St= Stomodium; Scale Bar= 100 μm.

## Neural Crest Cell Staining with HNK-1

HNK-1 is a mouse monoclonal antibody developed against quail ciliary ganglion and a human leukemic cell-line (Tucker et al.1984). HNK-1 labels migrating NCCs in avian embryos that are 1 to 3 days old. In addition to staining NCCs, nonspecific staining of neuroepithelial cells and neurons is observed in older animals (Tucker , 1984). As seen in Figure 9, HNK-1 labeled the NCCs migrating from the dorsal side of the neural

tube, thus providing an identification for NCCs and the opportunity to identify NCCs that were LIM3-positive via double staining. We observed that it also labeled the outer perimeters of the neural tube itself, the notochord, and some of the neuroepithelium as expected. Such labeling was not useful, however it did not interfere with interpretation.

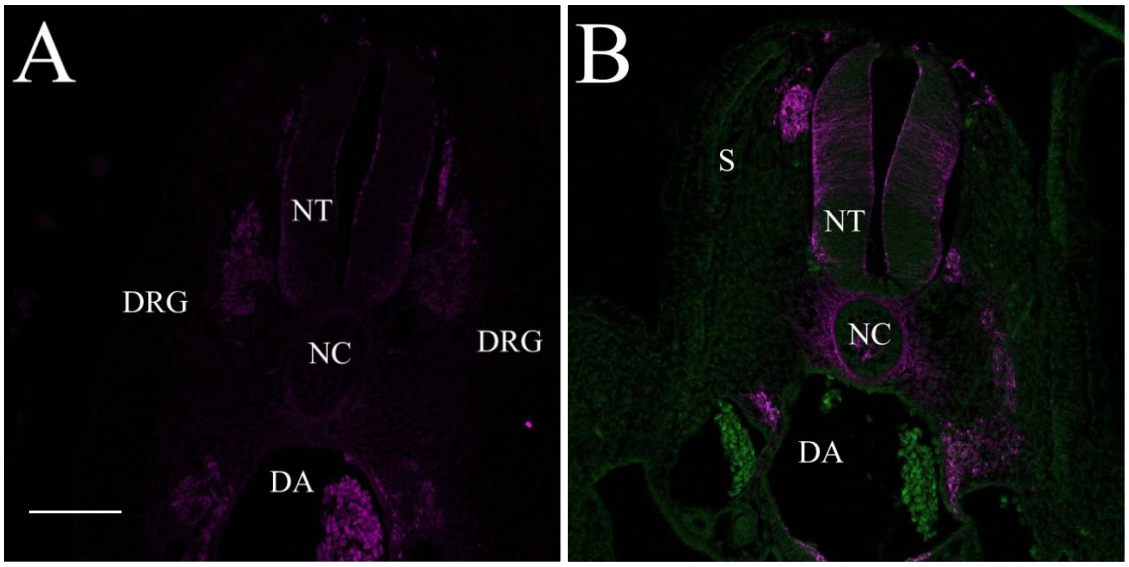


Figure 9. Sections through the trunk of HH stage 11-14 embryos labeled with monoclonal anti-LIM3 primary antibody, Alexafluor 488 secondary antibody, HKN-1 primary antibody and Alexafluor 594 secondary antibody. Images (A) and (B) show non-specific staining of HNK-1 on the neural tube, notochord, and other neuroepithelial structures. (A) A homocysteine treated embryo stained with only HNK-1 primary antibody and Alexfluor 594 secondary antibody. (B) The image is of a control embryo. This embryo was double stained with monoclonal anti-LIM3 primary antibody, Alexafluor 488 secondary antibody, HKN-1 primary antibody and Alexafluor 594 secondary antibody. NT= Neural Tube; NC= Notochord; DA= Descending Aorta; S= Somite; DRG= Dorsal Root Ganglion; Scale Bar= 100 μm.

Autofluorescence of Erythrocytes

Autofluorescence of erythrocytes is caused by the accumulation of Schiff base compounds conjugated on the cell surface (Stoya et al.2002). Schiff base compounds are intermediates that originate from the aldehydes derived from lipid peroxidation and from the amino groups of phospholipids (Stoya et al.2002).

As seen in Figure 10A and B, the red blood cells and NCCs differ in size, shape and pattern of fluorescence. Red blood cells are larger than NCCs, disc shaped and display a more consistent fluorescence. NCCs are known for having irregular, web-shaped cells due to their migratory activity. NCCs also exhibit a spotted pattern of fluorescence as a result of LIM3 expression in focal adhesions and the nucleus.

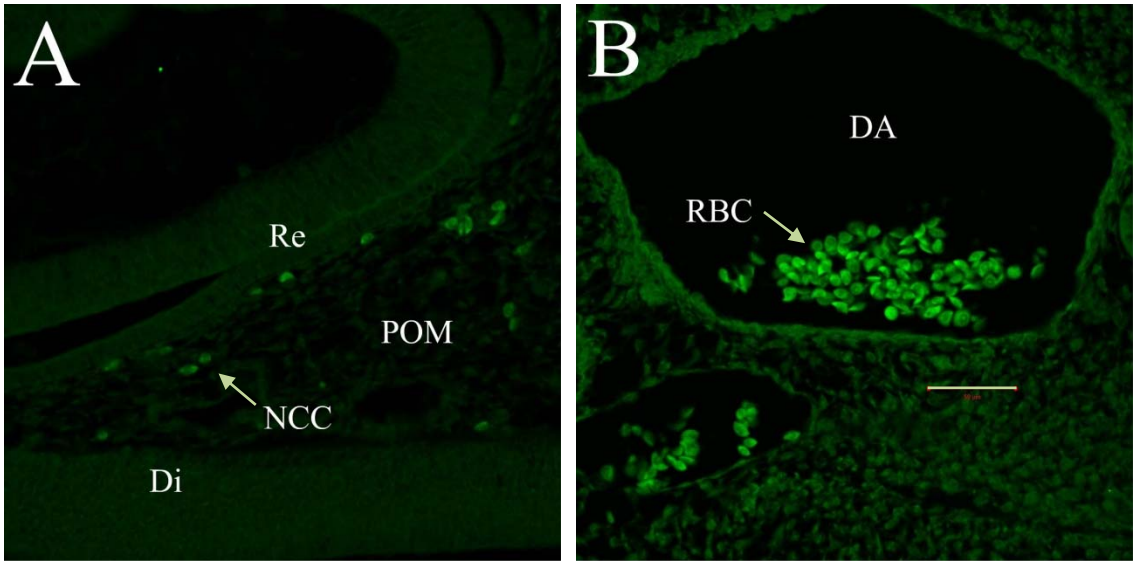


Figure 10. These sections have been labeled with monoclonal anti-LIM3 primary antibody and Alexafluor 488 secondary antibody. (A) is the eye of a control embryo. (B) is the dorsal aorta of a control embryo. POM= Periocular Mesenchyme; Re= Retina; Di= Diencephalon; NCC= Neural Crest Cells; DA= Dorsal Aorta; RBC= Red Blood Cells; Scale Bar= 50 μm.

# CHAPTER 4

# DISCUSSION

Hcys, an amino acid normally present in the blood, is a known terratogen causing primarily neural tube and cardiac outflow malformations when present at concentrations higher than normal in maternal blood. In a microarray study of the effect of Hcys on the mRNA expression from known genes, Rosenquist et al.(2007) found that many coding for proteins involved in cell adhesion and migration were altered by Hcys, suggesting that it exerts its teratogenic effects by perturbing NCCs as they migrate. One of these genes products is the LIM3 protein, a molecule of dual function, acting as a transcription factor and a focal adhesion protein. It was found to have expression 176 times greater than control level (Rosenquist et al.2007). In our study, chick embryos at HH stage 11-12 (40-50 hours of development, a time when NCC migration is getting well underway) were exposed to Hcys by injecting a solution of Hcys in saline (EBSS) into the amnion. They were exposed within the eggs for 24 hours of further development, advancing them to HH stage 17-18 (about 70 hours). Control embryos were treated identically but injected with the saline only. We identified neural crest cells in transverse sections of these embryos using the HNK-1 antibody and we identified and quantitatively measured the expression of LIM3 protein in the individual NCCs (HNK-1 positive) as well as in other positively staining cells. For this analysis, we chose three regions where NCC migration is known to be abundant and important for organ development: the paraxial region of mesenchyme near the spinal cord through which NCCs migrate and where some

aggregate to form the dorsal root ganglia, the mesenchyme near the optic cups where NCCs migrate en route to form the corneal endothelium, and the pharynx, through which NCCs migrate to form major thoracic arteries with associated connective tissues, and the aortico-pulmonary and truncal septa at the heart's outflow.

The primary antibodies used in this study were effective in labeling their specific target cells, as demonstrated by presence of intense staining of cells in the expected locations and the absence of staining in the negative controls (primary antibody omitted during the staining procedure), shown in Figure 1. After observing the cranial and cardiac sections of the chick embryos it was apparent that populations of neural crest cells emanate from the dorsal neural tube in successive waves. Multiple waves of migrating NCCs labeled with HNK-1 were often observed in the paraxial mesenchyme, as seen in Figures 8A and B. We observed positive cells in some sections of the predicted mesenchyme but absence of such staining in other sections through the same mesenchyme. Significantly, we also observed that not all HNK-1 labeled NCCs expressed LIM3 protein. Likewise, not all LIM3 protein expressing cells were double stained with HNK-1. This may indicate that the NCCs that do not express LIM3 protein may express it later on in development, but it also shows that Hcys is enhancing the LIM3 expression of many cells that are not NCCs, cells that may or may not contribute to known affected tissues and organs.

In paraxial mesenchyme surrounding the neural tube, the intensity of positively stained LIM3 cells was significantly greater in Hcys treated embryos than in the control

embryos. Our images show that in some sections the background staining was low but visibly variable, likely due to differences in section thickness. We controlled for variability by expressing all measured cell intensities as ratios—proportions of neural tube average intensity. The results support our hypothesis that elevated serum Hcys will increase the expression of LIM3 protein in NCCs. Hcys did not seem to affect the number of NCCs migrating into the paraxial mesenchyme labeled with HNK-1 nor the number of cells expressing LIM3 protein. Thus the effect was likely not re-directing differentiation of determined cells but was enhancing expression in cells already expressing LIM3.

The NCCs found in the periocular mesenchyme around the optic cup demonstrated a pattern of staining and intensity similar to that found in the paraxial mesenchyme. Generally, the cells of the treated embryos were observed to emit stronger intensities of LIM3 fluorescence compared to the control embryos. The results are consistent with our hypothesis that elevated plasma Hcys will cause an over-expression of LIM3 protein. If there were sequential waves of NCCs migrating into the periocular mesenchyme, it was not as apparent as it was in the paraxial mesenchyme. However, if the embryos were allowed more time to develop it may have been possible to observe multiple waves moving around the optic cup.

The number of NCCs observed in the pharynx region was smaller in comparison to the number in the paraxial and periocular mesenchyme. This may be because the chick embryos were only allowed to develop until HH stages 13-14, which may be too early in

development for a substantial number of NCCs to migrate into the pharynx. If the chick embryos were allowed to develop past HH stages 13-14 it is possible there would be more NCCs found in the tissue. The NCCs that were observed in the pharynx of the Hcys treated embryos exhibited stronger LIM3 expression than the control embryos. The findings support the hypothesis that elevated Hcys causes over-expression of LIM3 protein among NCCs. However, measuring the intensities of a greater number NCCs in the pharynx of a further developed embryo might reveal a more strongly supported result.

The findings are consistent with the concept that elevated maternal Hcys may alter the migration pattern of NCCs by causing them to over express LIM3 protein, thus affecting the focal adhesions and organization of the cytoskeleton. Past studies have suggested that neural tube defects and congenital heart defects can be induced by hyperhomocysteinemia (Rosenquist et al.1996; review by Steegers-Theunissen et al. 1991). In another study Rosenquist et al. showed that when NCCs were treated in vitro with exogenous Hcys, the genes affected were those corresponding to cell migration and adhesion, cellular metabolism, DNA and RNA interaction, and cell proliferation and apoptosis (Rosenquist 2007). Furthermore, Rosenquist et al.carried out a study in 2007 that identified the transcripts of genes of known function that were significantly altered by elevated Hcys. Of these genes, LIM3 mRNA was found to have increased to a level 176 times greater in Hcys treated embryos compared to the controls. Our findings are support and extend this finding.

In conclusion, our data and other studies are consistent with the idea that LIM3 protein has a role in assembling and organizing NCCs actin cytoskeleton during EMT, and show that elevated levels of Hcys magnify LIM3 expression. This offers a possible mechanism to explain at least in part how Hcys misguides development and leads to congenital embryonic neural tube and cardiovascular malformations.

REFERENCES

Aaku-Saraste E, Hellwig A, Huttner WB. Loss of Occludin and Functional Tight Junctions, but not ZO-1, during Neural Tube Closure—Remodeling of the Neuroepithelium Prior to Neurogenesis. Developmental Biology. 1996; 180(2): 664-679.

Akitaya T, Bronner-Fraser M. Expression of cell adhesion molecules during initiation and cessation of neural crest cell migration. Developmental dynamics. 1992; 194(1): 12-20.

Bard JB, Hay ED. The behavior of fibroblasts from the developing avian cornea. Morphology and movement in situ and in vitro. The Journal of Cell Biology. 1975; 67(2): 400-418.

Beebe DC, Coats JM. The lens organizes the anterior segment: specification of neural crest cell differentiation in the avian eye. Developmental Biology. 2000; 220(2): 424-431.

Bellairs R., Osmond M. Atlas of chick development. Academic Press. 2005.

Blom HJ, Smulders Y. Overview of Homocysteine and Folate Metabolism with special references to cardiovascular disease and neural tube defects. Journal of Inherited Metabolic Disease. 2011; 34(1): 75-81.

Bockman DE, Redmond ME, Kirby ML. Alteration of early vascular development after ablation of cranial neural crest. The Anatomical Record. 1989; 225(3): 209-217.

Boot MJ, Steegers-Theunissen RP, Poelmann RE, Van Iperen L, Lindemans J, Groot, GD, Adriana C. Folic acid and homocysteine affect neural crest and neuroepithelial cell outgrowth and differentiation in vitro. Developmental Dynamics. 2003; 227(2): 301-308.

Botto LD, Mulinare J, Erickson JD. Do multivitamin or folic acid supplements reduce the risk for congenital heart defects? Evidence and gaps. Am J Med Genet A. 2003 Aug 30; 121A(2): 95–101. [PubMed: 12910485]

Bronner-Fraser M. Mechanisms of neural crest cell migration. BioEssays. 1993; 15: 221-230.

Burstyn-Cohen T, Kalcheim C. Association between the cell cycle and neural crest delamination through specific regulation of G1/S transition. Developmental Cell. 2002; 3(3): 383-395.

Carlson BM. Human Embryology and Developmental Biology: with STUDENT CONSULT Online Access. Philadelphia (PA). WB Saunders Company. 2013.

Côté J, Turner CE, Tremblay ML. Intact LIM 3 and LIM 4 Domains of Paxillin Are Required for the Association to a Novel Polyproline Region (Pro 2) of Protein-Tyrosine Phosphatase-PEST. The Journal of Biological Chemistry. 1999; 274: 20550-20560. doi: 10.1074/jbc.274.29.20550.

Creuzet S, Couly G, Douarin NM. Patterning the neural crest derivatives during development of the vertebrate head: insights from avian studies. Journal of Anatomy. 2005; 207(5): 447-459.

Dorsky RI, Moon RT, Raible DW. Control of neural crest cell fate by the Wnt signalling pathway. Nature. 1998; 396: 370-373.

Edqvist PHD, Myers SM, Hallböök F. Early identification of retinal subtypes in the developing, pre-laminated chick retina using the transcription factors Prox1, Lim1, Ap2a, Pax6, Isl1, Isl2, Lim3 and Chx10. European Journal of Histochemistry. 2009; 50(2): 147-154.

Fitch J, Fini ME, Beebe DC, Linsenmayer TF. Collagen type IX and developmentally regulated swelling of the avian primary corneal stroma. Developmental Dynamics. 1998; 212(1): 27-37.

Garg V, Kathiriya IS, Barnes R, Schluterman MK, King IN, Butler C, Srivastava D. GATA4 mutations cause human congenital heart defects and reveal an interaction with TBX5. Nature. 2003; 424(6947): 443-447.

Hamburger V, Hamilton HL. A Series of Normal Stages in the Development of the Chick Embryo. Dev Dyn. 1992: 195(4); 231-272.

Hay ED. Development of the vertebrate cornea. Int Rev Cytol. 1980; 63, 263-322.

His W. Untersuchungen uber die erste Anlage des Wirbeltierleibes. Die erste Entwickelung des Hu hnchens im Ei. FCW Vogel, Leipzig. 1868.

Hobbs CA, Cleves MA, Karim MA, Zhao W, MacLeod SL. Maternal folate-related gene environment interactions and congenital heart defects. Obstetrics and Gynecology. 2010; 116(2 Pt 1): 316.

Hobbs CA, Cleves MA, Melnyk S, Zhao W, James SJ. Congenital heart defects and abnormal maternal biomarkers of methionine and homocysteine metabolism. American Journal of Clinical Nutrition. 2005; 81: 147-153.

Hoffman I, Balling R. Chromosomal localization of the murine cadherin-11. Mammalian Genome. 1995; 6(4): 304-304.

Hutson MR, Kirby ML. Neural Crest and Cardiovascular Development: a 20-Year Perspective. Birth Defects Res C Embryo Today. 2003; 69(1): 2-13.

Kaartinen V, Dudas M, Nagy A, Sridurongrit S, Lu MM, Epstein JA. Cardiac outflow tract defects in mice lacking ALK2 in neural crest cells. Development. 2004; 131(14): 3481-3490.

Khurana T, Khurana B, Noegel AA. Lim Proteins: Association with the Actin Cytoskeleton. Protoplasma. 2002; 219(1-2): 1-12.

Kirby ML. Cardiac Morphogenesis: Recent Research Advances. Pediatr Res. 1987; 21: 219-224.

Kirby ML, Gale TF, Stewart DE. Neural Crest Cells Contribute to Normal Aorticopulmonary Septation. Science. 1983; 220(4601): 1059-1061.

Kirby ML, Hutson MR. Factors controlling cardiac neural crest cell migration. Cell Adhesion & Migration. 2010; 4: 609 - 621; PMID: 20890117; http://dx.doi.org/10.4161/cam.4.4.13489

Kirby ML, Turnage KL 3rd, Hays BM. Characterization of Conotruncal Malformations Following Ablation of Cardiac Neural Crest. Anat Rec. 1985; 213(1): 87-93.

Kirby ML, Waldo KL. Role of neural crest in congenital heart disease. Circulation. 1990; 82(2): 332-340.

Kirby ML, Waldo KL. Neural crest and cardiovascular patterning. Circulation Research. 1995; 77(2): 211-215.

Lawson A, Anderson H, Schoenwolf GC. Cellular Mechanisms of Neural Fold Formation and Morphogenesis in the Chick Embryo. Anat Rec. 2001; 262: 153-168.

Le Douarin N. The Neural Crest. New York (NY): Cambridge University Press. 1982.

Le Douarin NM, Dupin E, Ziller C. Genetic and epigenetic control in neural crest development. Current Opinion in Genetics & Development. 1994; 4(5): 685-695.

Le Douarin NM., Ziller C, Couly GF. Patterning of Neural Crest Derivatives in the Avian Embryo: in Vivo and in Vitro Studies. Developmental Biology. 1993; 159(1): 24-49.

Marsot-Dupuch K, Smoker WRK, Grauer W. A Rare Expression of Neural Crest Disorders: An Intrasphenoidal Development of the Anterior Pituitary Gland. American Journal of Neuroradiology. 2004; 25: 285-288.

Martins-Taylor K, Schroeder DI, LaSalle JM., Lalande M., Xu RH. Role of DNMT3B in the regulation of early neural and neural crest specifiers. Epigenetics. 2012; 7(1): 71-82.

McCully KS. Vascular pathology of homocysteinemia: implications for the pathogenesis of arteriosclerosis. The American Journal of Pathology. 1969; 56(1): 111.

Milinsky A, Jick H, Jick SS. Multivitamin/folic acid supplementation in early pregnancy reduces the prevalence of neural tube defects. JAMA. 1989; 262: 2847-2852.

Miller AL. The methionine-homocysteine cycle and its effects on cognitive diseases. Altern Med Rev. 2003; 8(1): 7-19.

Minoux M, Rijli FM. Molecular mechanisms of cranial neural crest cell migration and patterning in craniofacial development. Development. 2010; 137: 2605–2621.

Miyagawa-Tomita S, Waldo K, Tomita H, Kirby ML. Temporospatial study of the migration and distribution of cardiac neural crest in quail-chick chimeras. American Journal of Anatomy. 1991; 192(1): 79-88.

Mwakikunga AR., Clubine AL, Wiens DJ. Homocysteine and Cardiac Neural Crest Cell Cytoskeletal Proteins in the Chick Embryo. International Journal of Biology. 2011: 3(2).

Nakagawa S, Takeichi M. Neural crest cell-cell adhesion controlled by sequential and subpopulation-specific expression of novel cadherins. Development. 1995; 121(5): 1321-1332.

Nakagawa S, Takeichi M. Neural crest emigration from the neural tube depends on regulated cadherin expression. Development. 1998; 125(15): 2963-2971.

Newgreen DF, Gooday D. Control of the onset of migration of neural crest cells in avian embryos. Cell and Tissue Research. 1985; 239(2): 329-336.

Nishiya N, Iwabuchi Y, Shibanuma M Côté, J, Tremblay ML, Nose K. Hic-5, a Paxillin Homologue, Binds to the Protein-tyrosine Phosphatase PEST (PTP-PEST) through Its LIM 3 Domain. The Journal of Biological Chemistry. 1999; 274: 9847-9853. doi: 10.1074/jbc.274.14.9847

Poelmann RE, Mikawa T, Groot GD. Neural crest cells in outflow tract septation of the embryonic chicken heart: differentiation and apoptosis. Developmental Dynamics. 1998; 212(3): 373-384.

Poelmann RE, Gittenberger-de Groot AC. A Subpopulation of Apoptosis-Prone Cardiac Neural Crest Cells Targets to the Venous Pole: Multiple Functions in Heart Development? Dev Biol. 1999; 207: 271-286.

Revel JP, Brown SS. Cell junctions in development, with particular reference to the neural tube. Cold Spring Harbor symposia on quantitative biology. Cold Spring Harbor (NY). Cold Spring Harbor Laboratory Press. 1976; 40: 443-455.

Rosenquist TH. Folate, Homocysteine and the Cardiac Neural Crest. Developmental Dynamics. 2013.

Rosenquist TH, Bennett GD, Brauer PR., Stewart M.L, Chaudoin TR, Finnell RH. Microarray analysis of homocysteine-responsive genes in cardiac neural crest cells in vitro. Developmental Dynamics. 2007; 236(4): 1044-1054.

Rosenquist TH, Chaudoin T, Finnell RH, Bennett GD. High-affinity folate receptor in cardiac neural crest migration: A gene knockdown model using siRNA. Developmental Dynamics. 2010; 239(4): 1136-1144.

Rosenquist TH, Finnell RH. Genes, folate and homocysteine in embryonic development. Proceedings of the Nutrition Society. 2001; 60: 53–61.

Rosenquist TH, Ratashak SA, Selhum J. Homocysteine induces congenital defects of the heart and neural tube: Effect of folic acid. Proceedings of the National Academy of Sciences USA. 1996; 93: 15227-15232.

Salvarezza SB, Rovasio RA. Exogenous retinoic acid decreases in vivo and in vitro proliferative activity during the early migratory stage of neural crest cells. Cell Proliferation. 1997; 30(2): 71-80.

Santiago A, Erickson CA. Ephrin-B ligands play a dual role in the control of neural crest cell migration. Development. 2002; 129: 3621-3632.

Sato M., Yost JH. Cardiac neural crest contributes to cardiomyogenesis in zebrafish. Developmental Biology. 2003; 257: 127-139.

Schoenwolf GC. The chick epiblast: a model for examining epithelial morphogenesis. Scanning Electron Microscopy. 1982: 3; 1371-1385.

Schoenwolf GC. Cell Movements Driving Neurulation in Avian Embryos. Development 2. 1991; (Suppl): 157-168.

Schoenwolf GC, Delongo J. Ultrastructure of secondary neurulation in the chick embryo. American Journal of Anatomy. 1980; 158(1): 43-63.

Shah NM., Groves AK, Anderson DJ. Alternative Neural Crest Cell Fates Are Instructively Promoted by TGFβ Superfamily Members. Cell. 1996; 85: 331-343.

Shah NM, Marchionni MA, Isaacs I, Stroobant P, Anderson DJ. Glial growth factor restricts mammalian neural crest stem cells to a glial fate. Cell. 1994; 77(3): 349-360.

Shaw GM., Selvin S, Carmichael SL, Schaffer DM, Nelson V, Neri E. Assessing combined chemical exposures as risk factors for neural tube defects. Reproductive Toxicology. 2001; 15(6): 631-635.

Soriano P. The PDGF alpha receptor is required for neural crest cell development and for normal patterning of the somites. Development. 1997; 124: 2691-2700.

Steegers-Theunissen RP, Boers GH, Trijbels FJ, Eskes TK. Neural-tube defects and derangement of homocysteine metabolism. N Engl J Med. 1991; 324(3): 199-200.

Stemple DL., Anderson DJ. Lineage Diversification of the Neural Crest: In Vitro Investigations. Developmental Biology. 1993; 159: 12-23.

Stoya G, Klemm A, Baumann E, Vogelsang H, Ott U, Linss W, Stein G. Determination of autofluorescence of red blood cells (RbCs) in uremic patients as a marker of oxidative damage. Clinical Nephrology. 2002; 58(3): 198-204.

Tanihara H, Sano K, Heimark RL, St. John T, Suzuki S. Cloning of five human cadherins clarifies characteristic features of cadherin extracellular domain and provides further evidence for two structurally different types of cadherin. Cell Communication and Adhesion. 1994; 2(1): 15-26.

Tierney BJ, Ho T, Reedy MV, Brauer PR. Homocysteine inhibits cardiac neural crest cell formation and morphogenesis in vivo. Developmental Dynamics. 2004; 229(1): 63-73.

Thompson RP, Fitzharris TP. Morphogenesis of the truncus arteriosus of the chick embryo heart: the formation and migration of mesenchymal tissue. American Journal of Anatomy. 1979; 154(4): 545-556.

Tucker GC, Aoyama H, Lipinski M, Tursz T, Thiery JP. Identical reactivity of monoclonal antibodies HNK-1 and NC-1: conservation in vertebrates on cells derived from the neural primordium and on some leukocytes. Cell Differentiation, 1984; 14(3): 223-230.

Vallin, J, Girault JM, Thiery JP, Broders F. Xenopus cadherin-11 is expressed in different populations of migrating neural crest cells. Mechanisms of Development. 1998; 75(1): 171-174.

Wagner C. "Biochemical Role of Folate in Cellular Metabolism." Folate in Health and Disease. 1995: 23-42.